Original Article

Global brain volume reductions in a sub-chronic phencyclidine animal model for schizophrenia and their relationship to recognition memory

Journal of Psychopharmacology
1–14

DOI: 10.1177/0269881119844196
journals.sagepub.com/home/jop

Nazanin Doostdar[1§], Eugene Kim[2§], Ben Grayson[1], Michael K Harte[1], Joanna C Neill[1*] and Anthony C Vernon[3,4*]

Abstract

Background: Cognitive deficits and structural brain changes co-occur in patients with schizophrenia. Improving our understanding of the relationship between these is important to develop improved therapeutic strategies. Back-translation of these findings into rodent models for schizophrenia offers a potential means to achieve this goal.

Aims: The purpose of this study was to determine the extent of structural brain changes and how these relate to cognitive behaviour in a sub-chronic phencyclidine rat model.

Methods: Performance in the novel object recognition task was examined in female Lister Hooded rats at one and six weeks after sub-chronic phencyclidine (2 mg/kg intra-peritoneal, n=15) and saline controls (1 ml/kg intra-peritoneal, n=15). Locomotor activity following acute phencyclidine challenge was also measured. Brain volume changes were assessed in the same animals using ex vivo structural magnetic resonance imaging and computational neuroanatomical analysis at six weeks.

Results: Female sub-chronic phencyclidine-treated Lister Hooded rats spent significantly less time exploring novel objects ($p<0.05$) at both time-points and had significantly greater locomotor activity response to an acute phencyclidine challenge ($p<0.01$) at 3–4 weeks of washout. At six weeks, sub-chronic phencyclidine-treated Lister Hooded rats displayed significant global brain volume reductions ($p<0.05$; $q<0.05$), without apparent regional specificity. Relative volumes of the perirhinal cortex however were positively correlated with novel object exploration time only in sub-chronic phencyclidine rats at this time-point.

Conclusion: A sustained sub-chronic phencyclidine-induced cognitive deficit in novel object recognition is accompanied by global brain volume reductions in female Lister Hooded rats. The relative volumes of the perirhinal cortex however are positively correlated with novel object exploration, indicating some functional relevance.

Keywords
Cognitive dysfunction, phencyclidine, rat, schizophrenia, magnetic resonance imaging, atrophy, behaviour

Introduction

Impairments in cognition are a core feature and a clinical unmet need in the treatment of schizophrenia and related psychoses (Bora and Pantelis, 2015; Bortolato et al., 2015). Cognitive deficits and negative symptoms have an adverse impact on quality of life (Green, 2006), bear a large socioeconomic cost and are refractory to current drugs for psychosis, including dopamine receptor (D2) antagonists such as haloperidol. Understanding the neural basis of impaired cognition in schizophrenia is therefore of significant importance (Cadinu et al., 2018). In parallel, structural brain abnormalities are also core features of schizophrenia and other serious neuropsychiatric disorders. In particular, reduced total brain and hippocampal volume, ventricular enlargement and thinning of the frontal and parietal-temporal cortical lobes, are the most commonly replicated findings in patients with schizophrenia, with robust effect sizes (Haijma et al., 2013; van Erp et al., 2016; van Erp et al., 2018). At least some of these anatomical abnormalities are present in non-medicated patients with schizophrenia, suggesting that abnormal brain structure is part of the disease pathophysiology and not solely the result of exposure to drugs for psychosis (Brugger and Howes, 2017). Whilst meta-analyses provide evidence for significant associations between frontal or temporal cortical thinning and positive and negative symptoms, respectively (Walton et al., 2017; Walton et al., 2018), there is evidence both for and against relationships between brain structure and cognitive performance in patients with schizophrenia. This most likely reflects heterogeneity in diagnosis, illness stage and the specific cognitive domains under investigation (Dempster et al., 2017; Heinrichs et al., 2017; Jirsaraie et al.,

[1]Division of Pharmacy and Optometry, School of Health Sciences, Faculty of Medicine, Biology and Health, University of Manchester, Manchester, UK
[2]Department of Neuroimaging, Institute of Psychiatry, Psychology and Neuroscience, King's College London, London, UK
[3]Department of Basic and Clinical Neuroscience, Institute of Psychiatry, Psychology and Neuroscience, King's College London, London, UK
[4]MRC Centre for Neurodevelopmental Disorders, King's College London, London, UK

[§]These authors contributed equally to this publication.
*Shared senior authorship.

Corresponding author:
Anthony C Vernon, King's College London, Institute of Psychiatry, Psychology and Neuroscience, Department of Basic and Clinical Neuroscience, Maurice Wohl Clinical Neuroscience Institute, 5 Cutcombe Road, London, SE5 9RT, UK
Email: anthony.vernon@kcl.ac.uk

2018; Karnik-Henry et al., 2012; Massey et al., 2017). As such, efforts to improve our understanding of these associations, have the potential to help uncover the neuronal substrates of impaired cognition and so facilitate the discovery of novel therapeutic targets.

Disturbances in glutamatergic and gamma-amino-butyric-acid neurotransmitter systems potentially induced by hypofunction of the N-methyl-d-aspartate receptor (NMDAR) remains a leading candidate mechanism for schizophrenia pathogenesis (Cadinu et al., 2018; Moghaddam and Javitt, 2012). This was derived partly from the early observation of reduced glutamate in the cerebrospinal fluid (CSF) of patients (Kim et al., 1980) and the finding that NMDAR antagonists, including ketamine and phencyclidine (PCP) robustly induce certain aspects of disease symptomatology in humans, including cognitive impairments (Krystal et al., 1994). Moreover, NMDAR antagonists exacerbate symptoms in schizophrenia patients that were otherwise stable on antipsychotic medication (Lahti et al., 1995a; Lahti et al., 1995b). Chronic intake of ketamine, at least in the context of addiction, is also reported to cause decreases in frontal lobe grey matter volume (Chesters et al., 2017; Liao et al., 2010) and abnormal white matter microstructure (Edward Roberts et al., 2014; Liao et al., 2011). NMDAR hypofunction therefore potentially contributes to abnormal brain structure and function as well as cognitive dysfunction in patients with schizophrenia. Back-translating these findings into rodents through the development of NMDAR antagonist rodent models (Cadinu et al., 2018; Moghaddam and Javitt, 2012; Pratt et al., 2012) therefore offers a potentially fruitful approach to investigate the associations between cognitive behaviour and brain structure, with full control of genetic and environmental factors and in the absence of confounds such as antipsychotic drug treatment. The administration of sub-chronic PCP (scPCP) has been widely reported by ourselves and others to induce both aspects of negative symptoms and cognitive impairments of relevance for schizophrenia, as reviewed extensively elsewhere (Cadinu et al., 2018; Neill et al., 2010; Neill et al., 2014; Pratt et al., 2012). We have also shown several pathological changes of relevance to the disorder in this model including reduced parvalbumin-positive interneurons and abnormal prefrontal dopamine levels during performance of the novel object recognition (NOR) task (Abdul-Monim et al., 2007; McLean et al., 2017; Reynolds and Neill, 2016).

In contrast, whilst several studies have elegantly demonstrated the impact of acute or scPCP treatment on rodent brain function using either pharmacological magnetic resonance imaging (phMRI) or semi-quantitative 2-deoxyglucose (2-DG) mapping of local cerebral glucose utilization (LGCU), in combination with functional connectivity network analyses (Dawson et al., 2010; Dawson et al., 2014; Dawson et al., 2015; Gozzi et al., 2008), we are the only group to have confirmed that scPCP induces MRI-detectable structural changes in the rodent brain with relevance for schizophrenia (Barnes et al., 2014). These included ventricular enlargement, decreased hippocampal volume and thinning of the frontal and parietal cortex (Barnes et al., 2014). In the same study, we reported that scPCP also induced significant deficits in sustained attention; however, the behavioural and magnetic resonance imaging (MRI) analyses were carried in separate cohorts of male rats. No studies have investigated whether these scPCP-induced structural brain deficits are transient, static or progress further with a longer duration of follow-up. Furthermore, no studies have explicitly tested for any relationship between abnormal brain anatomy and impaired cognition in this translational animal model. Therefore, we currently lack any evidence for the functional relevance of these apparent brain structural deficits as they relate to the model we have thoroughly validated in female rats. We use females for a variety of reasons explained elsewhere (see Cadinu et al. 2018 for a review of this topic). In the current study, we begin to address these gaps in our knowledge. Specifically, we examined the long-term effects of scPCP exposure (six weeks) on memory (using our well established NOR paradigm) and brain anatomy using high-resolution, *ex vivo* MRI, coupled with computational neuroanatomical analysis methods, as we have reported for other rodent models of relevance for schizophrenia (Crum et al., 2017; Hamburg et al., 2016; Richetto et al., 2017). Finally, we also tested for any correlations between measures of performance in NOR and regional brain volumes at this time-point.

Experimental procedures

Animals

All *in vivo* work including injections and behavioural testing was undertaken at the University of Manchester (performed by ND). Female Lister Hooded rats (n=30; Charles River, UK; weighing 194.3±2.24 g (mean±standard deviation (SD)) were housed in groups of five per cage in ventilated plastic cages (38 cm × 59 cm × 24 cm, GR1800 Double-Decker Cage, Tecniplast, UK) containing sawdust, paper sizzle nest and cardboard tunnels (Datesand group, UK) under a standard 12-hour light: dark cycle (lights on 07:00). The environment was maintained at 21±2° C, 55%±5% humidity.

Behavioural testing took place during the light cycle, under normal lighting (100 lux). Animals undergoing behavioural experiments had access to standard rat chow (Special Diet Services) and water *ad libitum* in the home cage. All experimental procedures were performed in accordance with the relevant guidelines and regulations, specifically, the Home Office (Scientific Procedures) Act 1986, United Kingdom and European Union (EU) directive 2010/63/EU. Furthermore, all work was carried out with the approval of the local Animal Welfare and Ethical Review Body (AWERB) panels at both the University of Manchester and King's College London (KCL).

scPCP administration

Phencyclidine hydrochloride was purchased from Sigma-Aldrich (P3029; Gillingham, Dorset, UK). Animals were administered saline (0.9% saline, n=15) or PCP (2 mg/kg, n=15) via the intraperitoneal (i.p.) route. The scPCP treatment regimen has been described many times and consisted of seven twice-daily (at approximately 09:00 and 17:00) injections followed by a seven-day washout period (Barnes et al., 2014, Neill et al., 2010, Neill et al., 2014). During this total 14-day period, animals received no behavioural testing and were handled only while receiving injections.

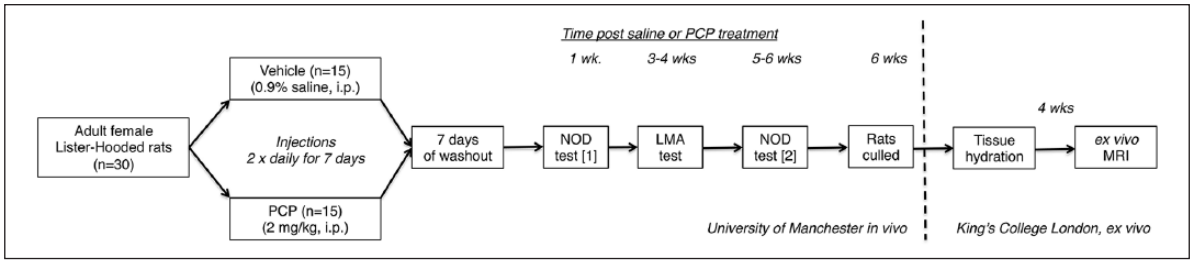

Figure 1. Experimental timeline. All in vivo animal work including drug treatment and behavioural analysis was carried out at the University of Manchester. Female Lister Hooded (LH) rats (*n*=30) were sub-chronically exposed to either phencyclidine (PCP) 2 mg/kg, intra-peritoneal (i.p.) (*n*=15) or 0.9% saline as a control (*n*=15), twice daily for seven days, followed by seven days washout. Animals were then tested in the novel object recognition (NOR) paradigm, also referred to as Novel object detection (NOD) after one and six weeks of drug-washout. Locomotor activity (LMA) in response to acute saline or PCP challenge was examined in all animals in each group using a crossover design after three weeks of drug washout. Animals were culled after the final behavioural session and brain tissue prepared and shipped to King's College London (KCL) for ex vivo magnetic resonance imaging (MRI) after four weeks hydration in 0.01M phosphate buffer containing 0.05% w/v sodium azide and 2% v/v Magnevist gadolinium-based contrast agent.

Experimental design

A summary of the timeline of experimental procedures is shown in Figure 1. After the seven-day washout period, saline and PCP-treated rats underwent behavioural testing in the NOR paradigm twice, once at one week post-dosing and again at six weeks post-dosing. All animals also underwent a locomotor activity (LMA) test, three weeks post-dosing to confirm successful scPCP treatment. All animals were culled 24 h after the final NOR test to enable *ex-vivo* magnetic resonance imaging to be carried out.

Behavioural apparatus and testing

NOR testing was conducted in open Plexiglas boxes (52 cm W, 52 cm L, 30 cm H). Each box consisted of black walls and a white floor divided into nine square sectors. The objects used in the NOR consisted of Coca-Cola cans and brown medicine bottles, as previously described in detail by us (Grayson et al. 2007). Two days prior to the first NOR test, rats were placed in the testing box with their cage-mates for 15 min. On the following day, rats were allowed 10 min to explore the NOR test box individually. On the test day, rats were placed in the NOR box to explore two identical objects for three minutes (acquisition phase). Rats were then removed from the NOR box and placed into an unfamiliar Plexiglas box (24 cm W, 44 cm L, 19 cm H) for a one-minute inter-trial-interval (ITI). Following this, rats were returned to the NOR box to explore a novel object and a replica of the familiar object for three minutes (retention phase). The NOR box and all objects were cleaned with 70% ethanol at the end of each NOR testing session to remove olfactory trails. All experiments were filmed and video-recorded for subsequent analysis by an experienced blinded experimenter. Object exploration time in each phase of the task was scored using the 'Jack Rivers-Auty' online stopwatch (http://jackrrivers.com/program/). Object exploration was defined as licking and sniffing of the object whilst leaning on or touching the object. Turning towards and sitting on or next to the object without sniffing was not considered exploration (Grayson et al., 2007; Grayson et al., 2015). The discrimination index (DI) was also calculated, defined as (time exploring novel object (s) – time exploring familiar object (s))/(time exploring novel object (s) + time exploring familiar object (s)). LMA was also evaluated by counting the total number of lines crossed by the rat in both the acuqisiton and retention phase. The LMA response to acute PCP challenge was monitored in automated testing chambers (Photobeam Activity system, San Diego instruments). The testing chambers were translucent Plexiglas boxes (24 cm W, 44 cm L, 19 cm H) with a perforated translucent Plexiglas lid (to allow air flow). All chambers were controlled using Pas764 LMA software to record the number of interruptions to the photo beam within the chamber. Rats were habituated to the LMA chambers one day prior to testing, which involved leaving individual rats in the LMA chamber for one hour. On the day of testing, rats were placed in the LMA chambers and baseline activity levels were monitored every five minutes for 30 min. Rats were then treated with an acute dose of vehicle (0.9% saline; i.p.) or PCP (2 mg/kg; i.p.) and placed back into the testing chamber to be monitored every five minutes over 60 min. LMA testing was conducted over two weeks with a cross over in the treatment groups so that all rats received both vehicle and PCP.

Tissue preparation for ex vivo *MRI*

Saline (*n*=15) and scPCP (*n*=15) treated-rats were culled by cardiac perfusion (0.9% saline followed by 4% paraformaldehyde) under terminal anaesthesia (sodium pentobarbital, 60 mg/kg i.p.) and prepared for *ex vivo* MRI at the University of Manchester as described elsewhere (Vernon et al., 2011). In brief, fixed brain tissues were kept intact in the cranium and post-fixed for 12 h in 4% paraformaldehyde. Samples were then shipped to KCL and on arrival transferred into 0.01M phosphate buffer containing 0.05% w/v sodium azide and 2 mM Magnevist (Bayer Plc) for four weeks prior to MRI. We did not conduct a formal power analysis to establish sample sizes. However, our final group size (*n*=15) per group is larger than the only prior structural neuroimaging study in the scPCP rat model (Barnes et al., 2014).

MRI acquisition

A 9.4T horizontal small bore magnet (Bruker Biospec; Bruker BioSpin GmbH, Germany) and a quadrature volume

radiofrequency coil (39 mm internal diameter, RAPID Biomedical GmbH, Germany) were used for all MRI acquisitions. Fixed brain samples were placed securely one at a time in a custom-made magnetic resonance (MR)-compatible holder and immersed in proton-free susceptibility matching fluid (FluorinertTM FC-70; Sigma-Aldrich). Samples were scanned in a random order, with the KCL operator (ACV) blinded to treatment group (saline or PCP) by numerical coding of samples undertaken at the University of Manchester (performed by ND). Scanning of samples was interspersed with phantoms to ensure consistent operation of the scanner. From each animal a single 3D fast-spin echo (FSE) image was acquired for brain structural analyses, with the following parameters: Echo time / repetition time=30/300 ms, echo train length=4, number of averages=2, matrix size=375×225×225 and field of view (FOV)=30 mm × 18 mm × 18 mm, yielding isotropic voxels of 80 μm. Total scan-time was two hours, six minutes per brain.

MR image analysis

The raw MR images were downloaded from the scanner server and converted to the Neuroimaging Informatics Technology Initiative image file format, inspected for artefacts and then pre-processed as described previously (Wood et al., 2016) (performed by EK). After a quality control inspection, one scan in the scPCP group was excluded due to mechanical injury to the brain sustained during sample preparation. The final *n* values per group for statistical comparisons of MRI data were therefore *n*=15 saline and *n*=14 scPCP. A study template image was constructed using the 3D FSE MR images from the whole dataset to avoid bias (*n*=29). The resulting 3D FSE template was then non-linearly registered to two open access rat MRI atlases, the Waxholm space Sprague-Dawley rat brain atlas (Papp et al., 2014) and the rat cortical *in vivo* MRI Template (Valdes-Hernandez et al., 2011). This approach combines the best features of these two atlases, with excellent subcortical and cortical parcellation, respectively. MR images from individual animals were then non-linearly registered to this study template using their T2-weighted FSE images. Logarithmic Jacobian determinants (*J*) were calculated from the inverse warp fields in standard space to estimate apparent volume change (Crum et al., 2017; Vernon et al., 2014; Wood et al., 2016).

Statistical analysis

Behavioural data

Statistical analyses on all behavioural datasets were performed using Prism software (v7.0; Graph Pad Software Inc., La Jolla, California, USA). Data were first confirmed as normally distributed using a combination of the Kolgorov-Smirnov normality test and D'Agostino and Pearson omnibus normality test. For the NOR task, group-level differences between saline (*n*=15) and PCP-exposed rats (*n*=15) with object exploration time as the dependent variable were assessed using a two-tailed *t*-test, with α=0.05 for each phase of the task separately. Group-level differences using the DI as the dependent variable were also assessed using a two-tailed *t*-test, with α=0.05. LMA, defined as total number of lines crossed in both the acquisition and retention phases of the NOR tasks, was also calculated and compared between saline and PCP-exposed animals using a two-tailed *t*-test, with α=0.05. In the LMA test, a 2×2 repeated measures analysis of variance (ANOVA) with 'time' as within-subject factor (and repeated measure) and 'treatment' as between-subject factor was used to assess group-level differences between saline and PCP-exposed animals using total distance moved as the dependent variable. *Post-hoc* tests (Bonferroni, corrected for multiple comparisons) were performed for any significant time×treatment interactions arising from the 2×2 ANOVA model, with α=0.05. An area under the curve (AUC) analysis was also carried out for total distance moved in each group, analysed using one-way ANOVA with *post-hoc* Bonferroni test (corrected for multiple comparisons, with α=0.05.

MR image analysis

We employed a combination of atlas-based segmentation (ABS) and voxel-wise tensor-based morphometry (TBM) analyses (Crum et al., 2017). In the ABS approach, we took advantage of two freely available rat MRI atlases. First, the Waxholm MRI atlas, which is parcellated into *n*=80 regions of interest (ROIs) that are predominantly sub-cortical, including hippocampal subfields as well as the olfactory system and cerebellum (Papp et al., 2014). Second, the rat cortical *in vivo* MRI atlas, which is parcellated into *n*=47 exclusively cortical ROIs (Valdes-Hernandez et al., 2011). The ROIs of the Waxholm MRI atlas were transformed to the rat cortical *in vivo* MRI atlas space via non-linear registration of the respective template images. This combination therefore allows an in-depth exploration of both sub-cortical and cortical volumes in the rat brain that is not possible using either atlas alone. From this combined atlas, we successfully extracted values for volume (mm^3) from 72/80 ROIs in the Waxholm atlas, (missing ROIs: optic nerve, inner ear, commissural stria terminalis, central canal, spinal trigeminal tract, frontal association cortex, habenular commissure, nucleus of the stria medullaris and medial lemniscus decussation) and 45/47 ROI in the rat cortical atlas (missing ROIs: dorsal intermediate entorhinal cortex (DIEnt) and medial entorhinal cortex (MEnt)). Total brain volumes were also calculated. In total, we therefore obtained volume measurements from *n*=117 brain ROIs per animal, per treatment group. Group-level differences contrasting saline (*n*=15) vs scPCP (*n*=14) using volume (mm^3) as the dependent variable were then performed using two-tailed t-tests, corrected for multiple comparisons using the false discovery rate (FDR) procedure of Benjamini and Hochberg with a 0.05 (5%; $q<0.05$) threshold (Genovese et al., 2002). The same statistical analyses were run for both absolute volumes and relative volumes, the latter calculated by expressing individual absolute ROI volumes as a percentage of total brain volume (Crum et al., 2017). This approach also controls for potentially spurious volume differences emerging due to overall between group-differences in total brain volume, reflecting the tight correlation between volumes of a structure and total brain volumes (Lerch et al., 2012). To complement and extend the ABS approach, we also carried out a voxel-wise tensor based morphometry (TBM) analysis of apparent volume change from the log-scaled Jacobian determinant maps, using permutation tests and threshold-free cluster enhancement (TFCE) in FSL randomise, corrected for multiple comparisons by controlling the family-wise error

(FWE) rate as described elsewhere (Crum et al., 2017; Vernon et al., 2014; Wood et al., 2016). As for the ABS, we ran this analysis both with and without total brain volume as a regressor of no interest in the design matrix.

Correlations between brain volume and behaviour

To assess the potential functional relevance of brain volume changes in scPCP-treated rats, we examined the degree of correlation between parameters measured in the NOR task at six weeks and the volume of *a priori* selected brain regions, previously reported as neural correlates of performance in the NOR task as described below. Data were first confirmed as normally distributed using a combination of the Kolgorov-Smirnov normality test and D'Agostino and Pearson omnibus normality test. Pearson product moment (two-tailed) correlations were then run comparing exploration time (s) for novel and familiar objects and the DI, in the NOR task at week 6, against the volumes (both absolute and relative) of the cingulate cortex (Weible et al., 2009), perirhinal cortex, split into areas 35 and 36 (Brown and Aggleton, 2001; Gilbert and Kesner, 2003; Kinnavane et al., 2016; Morillas et al., 2017; Peters et al., 2018; Winters et al., 2008), postrhinal cortex, cornu ammonis (CA) 1, 2 and 3 and the dentate gyrus (Brown and Aggleton, 2001; Chang and Huerta, 2012; Winters et al., 2008) for all animals in each group (scPCP or vehicle) separately. Correlations were only performed for animals where both behavioural and MRI data were available (saline, n=15; scPCP, n=14). Significance was set at $p<0.05$. As these are exploratory correlations we did not perform corrections for multiple comparisons.

Results

scPCP impairs performance in the NOR paradigm in female Lister Hooded rats after a seven-day washout

In the acquisition phase, both vehicle and PCP-exposed rats spent similar time exploring the identical objects (Figure 2(a)). In the retention phase, saline-treated animals spent significantly more time exploring the novel object ($p<0.05$), whilst scPCP-treated animals explored both objects equally (Figure 2(b)). The DI was clearly reduced in scPCP rats compared to vehicle controls, but this failed to reach statistical significance (p=0.1; Figure 2(c)). Total LMA did not differ significantly across both phases of testing between saline and scPCP-treated rats (p=0.54; Figure 2(d)).

scPCP leads to sustained deficits in the NOR paradigm in female Lister Hooded rats up to six weeks post-exposure

To confirm if the observed deficits in the NOR paradigm at one week post-dosing are sustained, rats were re-tested in this paradigm after an additional five weeks from the cessation of PCP or saline treatment (six weeks in total from the end of PCP treatment). In the acquisition phase, there were no differences between vehicle and scPCP-treated rats, which spent similar times exploring the identical objects (Figure 2(e)). In the retention phase saline, but not scPCP-treated rats spent more time investigating the novel object ($p<0.05$; Figure 2(f)). The DI was clearly reduced in scPCP rats compared to vehicle controls, but this failed to reach statistical significance (p=0.07; Figure 2(g)). No significant differences in LMA were detected across both phases of testing between saline and scPCP-treated rats, although this trended towards a reduction in the scPCP group (p=0.052; Figure 2(h)).

Increased total LMA following PCP-challenge in female Lister Hooded rats previously exposed to sub-chronic PCP but not saline

In a crossover design, all rats in either the saline or scPCP groups were tested for total LMA after a saline or PCP (2 mg/kg) challenge, 3–4 weeks after the initial scPCP or vehicle treatment. Two-way repeated measures ANOVA of total LMA confirmed significant main effects of time (F(17,952)=57.3; $p<0.0001$), treatment (F(3,56)=4.89; $p<0.01$) and time×treatment interaction (F(51,952)=8.44; $p<0.0001$). *Post-hoc* testing on the interaction term confirmed that total LMA was higher in the scPCP exposed animals, following acute PCP challenge in comparison to all other treatment groups between 25–55 min after the challenge (55–80 min from the beginning of the experiment; Figure 2(i)). A one-way ANOVA analysis of the AUC for total LMA also found a significant overall difference across treatment groups (F(3,56)=8.07; $p<0.0001$). *Post-hoc* testing confirmed that the AUC for total LMA was significantly higher for the scPCP group challenged with scPCP compared to all other groups ($p<0.01$; Figure 2(j)).

scPCP results in sustained apparent global brain volume reductions without regional specificity

Six weeks after cessation of treatment, the total brain volumes of scPCP-treated rats were significantly reduced by –14.7% compared to saline controls (t=2.51; df=28; $p<0.05$; Cohen's d=0.84; Figure 3). Using our hybrid MRI atlas of the rat brain, ABS revealed that the absolute volumes of 115/117 (98%) atlas ROIs were significantly reduced in scPCP-treated rats compared to saline controls after FDR correction at $q<0.05$ (Supplementary Material Table 1). Effect sizes ranged from d=1.06 in the posterior parietal cortex (PtPC) to d=0.40 (ascending fibres of the facial nerve). There were no ROIs showing a positive volume increase in the scPCP group relative to saline controls. The ROIs with the largest effect sizes were PtPC (d=1.06); commissure of the superior colliculus (d=1.06) and anterior commissure (d=1.01). Only 2/117 (2%) of atlas ROIs were not significantly different between the groups, these being the genu and ascending fibres of the facial nerve (Supplementary Material Table 1). To check if these effects are a function of the global brain volume reduction in scPCP-treated rats, we repeated the ABS analysis using data corrected for total brain volume (relative volumes). In this analysis, only the relative volumes of 7/117 (6%) of the atlas ROIs were different when comparing scPCP-treated rats to vehicle controls and only then at trend-level significance ($p<0.05$ uncorrected), with no results surviving correction for multiple comparisons at $q<0.05$ (Supplementary Material Table 2).

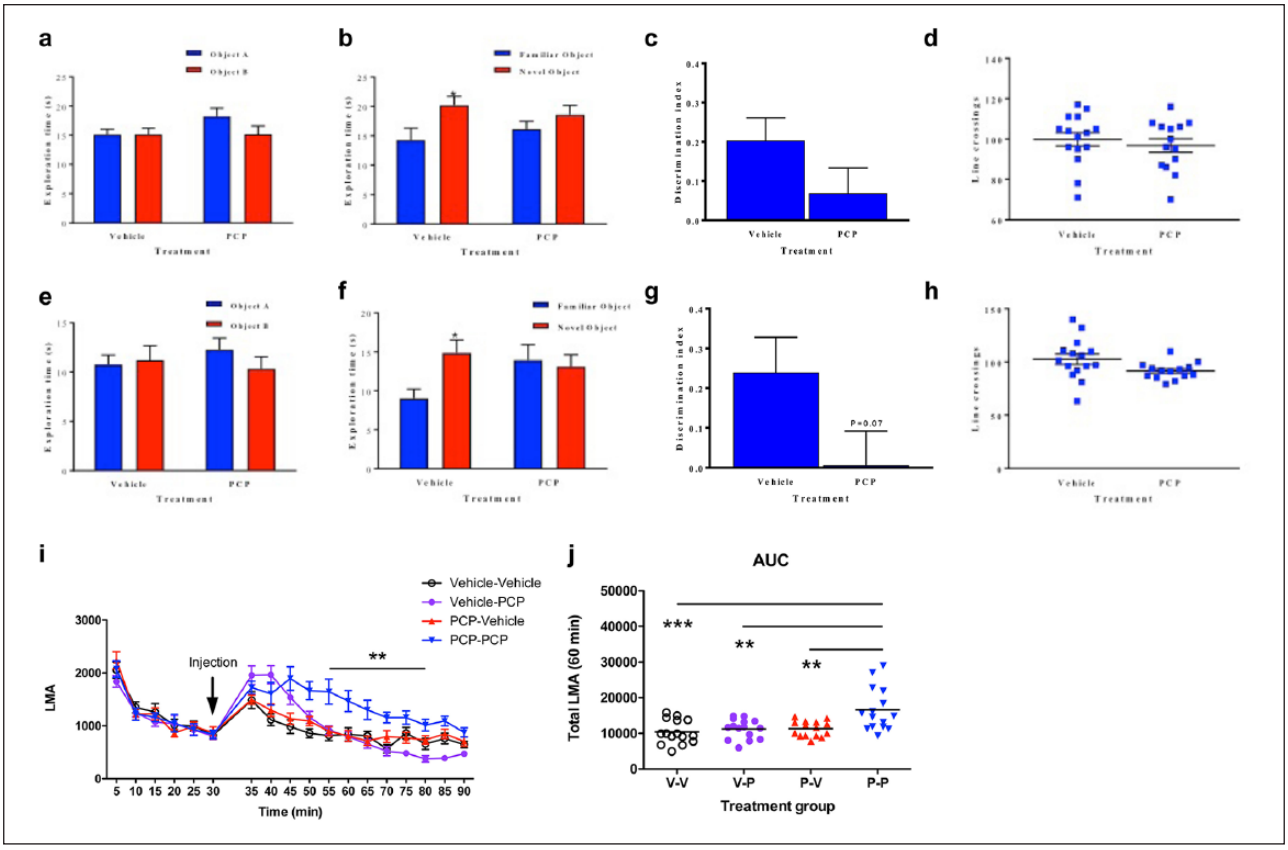

Figure 2. The effect of sub-chronic phencyclidine (PCP) (2 mg/kg, intraperitoneal (i.p.) twice daily for seven days, followed by a seven-day washout period) on the exploration time (s) of two identical objects, A and B, at one and six weeks after cessation of PCP treatment in the three-minute acquisition trial (Figure 2(a) and (e)) and the familiar object and a novel object in the three-minute retention trial (Figure 2(b) and (f)). Data for the discrimination index (DI) are also shown (Figure 2(c) and (g)). Data are expressed as mean±standard error of the mean (s.e.m.) (n=15 per group) and were analysed by Student's t-test. *$p<0.05$; significant difference between time spent exploring the familiar and novel object. There were no significant differences in the total number of line crossings in the acquisition plus retention trial as a measure of locomotor activity (LMA) at either time-point (Figure 2(d) and (h)). Data shown are scatterplot plus mean where each data point represents the LMA for an individual animal. Acute PCP challenge elicits significantly greater locomotor activity (LMA) as shown by the time course (Figure 2(i)) and area under the curve analysis (Figure 2(j)) following sub-chronic exposure to PCP as compared to saline-treated rats. In Figure 2(i), **$p<0.01$; PCP-PCP (n=15) vs all other treatment groups (all n=15; Bonferroni *post-hoc* test corrected for multiple comparisons on significant time×treatment interaction from 2×2 repeated measures (RM) analysis of variance (ANOVA)). In Figure 2(j), **$p<0.01$; ***$p<0.001$ PCP-PCP (P-P; n=15) vs all other treatment groups (all n=15; Bonferroni *post-hoc* test corrected for multiple comparisons following overall significant one-way analysis of variance (ANOVA) model). AUC: area under the curve; V-V: vehicle-vehicle; V-P: vehicle-PCP; P-V: PCP-vehicle; P-P: PCP-PCP.

Of these, the relative volume of the granule cell level of the cerebellum was modestly increased (+2.6%; Cohen's d=1.14), whereas the relative volumes of the other six atlas ROIs were reduced in scPCP treated animals by 2–3% with effect sizes in the range of d=0.77–1.08 (Supplementary Material Table 2).

To confirm and extend these data, we next performed voxel-wise TBM analysis, since this may be more sensitive than ABS to subtle apparent volume differences between the treatment groups (Crum et al., 2017; Lerch et al., 2008b; Sawiak et al., 2009b). TBM analysis without whole brain volume as a covariate revealed widespread clusters of voxels that were significantly smaller (FWE-corrected $p<0.05$) in scPCP-treated rats as compared to vehicle controls (Figure 4). These were widely distributed across the rat brain, affecting almost all major structures including the cortex as a whole, the basal ganglia, hippocampal formation, hypothalamus, basal forebrain and ventral midbrain. In contrast, in the cerebellum, only the upper layers appeared to be affected by scPCP-treatment (Figure 4). No voxels were larger in scPCP-treated rats as compared to vehicle controls (Figure 4). To confirm whether these apparent volume changes reflected the global change in brain volume in scPCP rats, we repeated the TBM analysis using total brain volume as a covariate. In this analysis, no clusters of voxels were either significantly smaller or larger when comparing scPCP and saline groups after FWE correction, even at highly exploratory statistical thresholds ($p<0.2$; data not shown). Taken together these data suggest apparent global, rather than local or region-specific effects of scPCP on female Lister Hooded rat brain volume six weeks post-exposure.

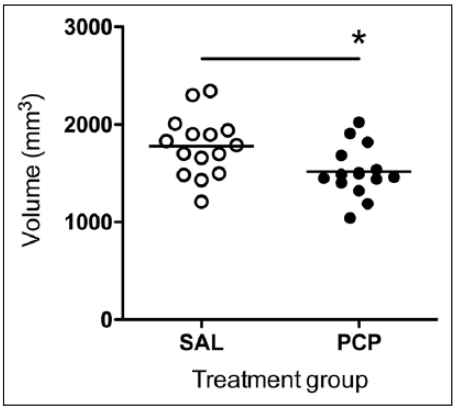

Figure 3. Total brain volume is significantly reduced in female Lister Hooded (LH) rats sub-chronically exposed to phencyclidine (PCP) (n=15) as compared to saline (SAL)-treated rats (n=15), six weeks post-exposure. *$p<0.05$ saline vs sub-chronic phencyclidine (scPCP), two-tailed t-test. Data shown are volumes (mm^3).

Correlation between the volumes of a priori brain ROIs and NOR performance at six weeks post-scPCP

In the vehicle control group, we found no significant correlations between the volumes of our *a priori* selected brain ROIs (using either absolute or relative volumes) and the behavioural measures from the NOR task performed six weeks post-treatment (Table 1). In contrast, in the scPCP group, we found a positive correlation at trend-level significance ($p<0.05$ uncorrected for multiple comparisons) between the relative volumes of the perirhinal cortex areas (PA) 35 and 36 and the time spent exploring the novel object (Table 2). Plotting the data revealed that scPCP rats with larger volumes of these regions spent more time exploring the novel object, with no such relationship observed in the control group (Figure 5). We did not run correlations to the NOR task at week 1 or LMA at week 3 since these were temporally separated from the MRI time-point.

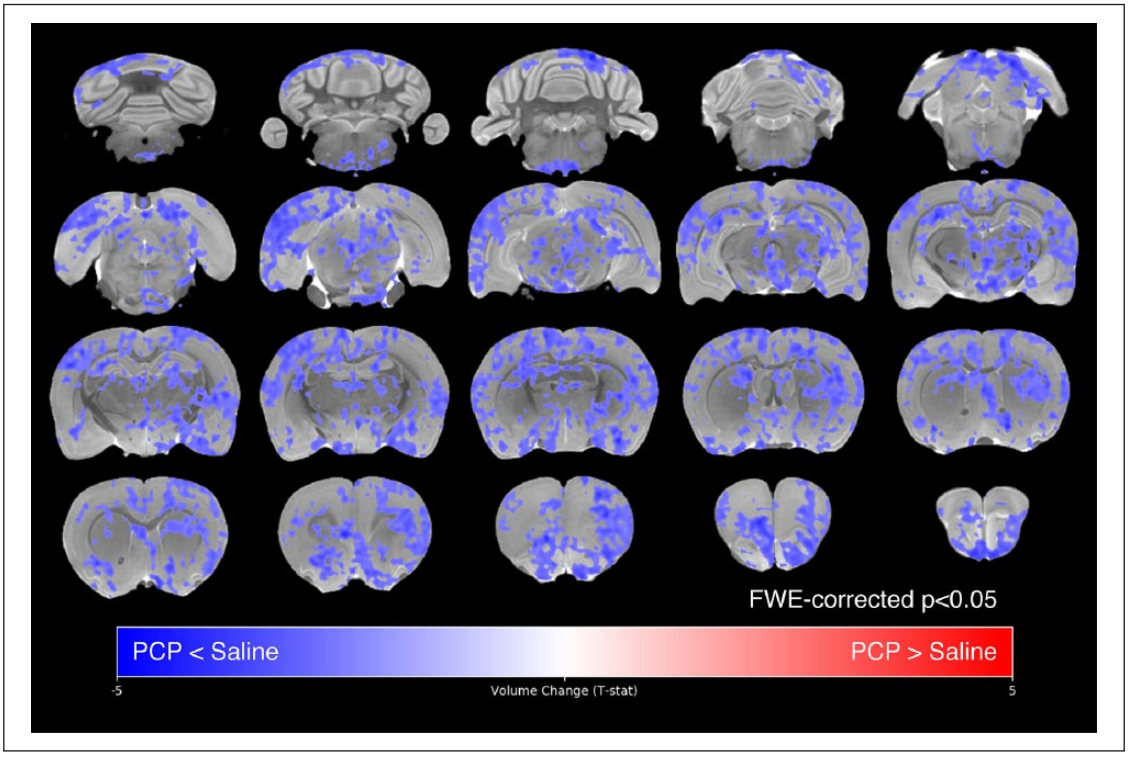

Figure 4. Voxel-wise tensor-based morphometry (TBM) analysis (not covarying for whole brain volume) reveals widespread apparent volume changes in the female rat brain six weeks after sub-chronic exposure to phencyclidine (PCP) as compared to saline controls. Data shown are voxel-wise t-statistics of group-levels differences (contrast: saline (n=15) vs PCP (n=15]) in the log scaled Jacobian determinant (J), corrected for multiple comparisons using family-wise error (FWE) with a 5% threshold ($p<0.05$), overlaid on the minimum deformation template image. Cold colours indicate apparent volume contraction (PCP< Saline). Note that co-varying for total brain volume results in no significantly different voxels between saline and scPCP-treated rats even at highly liberal and exploratory FWE thresholds (20%; $p<0.2$; *data not shown*) suggesting a lack of regional specificity in scPCP-induced volume changes in female LH rats.

Table 1. Correlations between behavioural data from the novel object recognition (NOR) task and magnetic resonance imaging (MRI)-derived volumes of *a priori* selected brain regions suggested to reflect the neural correlates of performance in this task in vehicle-treated rats (n=15), six weeks post-treatment.

Vehicle	Exploration time (s) Novel object		Exploration time (s) Familiar object		Discrimination index (DI)	
Atlas ROI	*Pearson's r*	*p-value*	*Pearson's r*	*p-value*	*Pearson's r*	*p-value*
Whole brain volume	–0.092	0.372	0.270	0.165	–0.231	0.204
Cornu ammonis 1 (CA1)	–0.101	0.360	0.238	0.197	–0.210	0.227
CA1 (%)	–0.068	0.405	–0.304	0.136	0.211	0.225
Dentate gyrus (DG)	–0.109	0.350	0.221	0.214	–0.205	0.232
DG (%)	–0.121	0.333	–0.369	0.088	0.189	0.249
Cornu ammonis 2 (CA1)	–0.073	0.398	0.257	0.178	–0.216	0.220
CA2 (%)	0.166	0.277	–0.186	0.253	0.189	0.250
Cornu ammonis 3 (CA1)	–0.084	0.383	0.282	0.154	–0.243	0.191
CA3 (%)	0.035	0.450	–0.063	0.412	–0.007	0.491
Postrhinal cortex (PRC)	–0.090	0.374	0.209	0.228	–0.166	0.277
PRC (%)	–0.044	0.438	–0.219	0.216	0.229	0.206
Perirhinal area (PA) 35	–0.116	0.340	0.235	0.200	–0.212	0.225
PA35 (%)	–0.208	0.228	–0.152	0.294	0.061	0.414
Perirhinal area (PA) 36	–0.099	0.363	0.236	0.199	0.198	0.239
PA36 (%)	–0.113	0.345	–0.195	0.243	0.172	0.270
Entorhinal cortex (EC)	–0.095	0.369	0.193	0.245	0.174	0.267
EC (%)	–0.071	0.401	–0.217	0.219	0.133	0.318
Cingulate cortex (Cg)	–0.043	0.440	0.371	0.086	–0.256	0.179
Cg (%)	0.144	0.304	0.437	0.052	–0.165	0.279

Data shown are correlation coefficients (Pearson's r) and p-values (two-tailed t-test) for both absolute and relative volumes (mm^3).

Table 2. Correlations between behavioural data from the novel object recognition (NOR) task and magnetic resonance imaging (MRI)-derived volumes of *a priori* selected brain regions suggested to reflect the neural correlates of performance in this task in sub-chronic phencyclidine (scPCP)-treated rats (n=14), six weeks post-treatment.

scPCP	**Exploration time (s) Novel object**		**Exploration time (s) Familiar object**		**Discrimination index (DI)**	
Atlas ROI	*Pearson's r*	*p-value*	*Pearson's r*	*p-value*	*Pearson's r*	*p-value*
Whole brain volume	0.098	0.370	0.233	0.211	–0.134	0.324
Cornu ammonis 1 (CA1)	0.110	0.353	0.262	0.182	–0.144	0.312
CA1 (%)	–0.009	0.487	0.092	0.377	–0.015	0.479
Dentate gyrus (DG)	0.109	0.355	0.265	0.180	–0.151	0.303
DG (%)	0.129	0.330	0.309	0.141	–0.152	0.302
Cornu ammonis 2 (CA1)	0.080	0.393	0.247	0.198	–0.158	0.295
CA2 (%)	–0.280	0.166	–0.023	0.469	–0.179	0.271
Cornu ammonis 3 (CA1)	0.059	0.420	0.237	0.207	–0.155	0.299
CA3 (%)	–0.299	0.150	0.123	0.337	–0.226	0.219
Postrhinal cortex (PRC)	0.034	0.454	0.277	0.169	–0.201	0.246
PRC (%)	–0.356	0.106	0.264	0.181	–0.378	0.091
Perirhinal area (PA) 35	0.167	0.284	0.242	0.202	–0.111	0.352
PA35 (%)	**0.631**	**0.008**	0.220	0.225	0.114	0.349
Perirhinal area (PA) 36	0.142	0.314	0.258	0.187	–0.137	0.320
PA36 (%)	**0.488**	**0.038**	0.291	0.156	–0.038	0.448
Entorhinal cortex (EC)	0.050	0.432	0.282	0.165	–0.198	0.249
EC (%)	–0.190	0.257	0.297	0.151	–0.338	0.119
Cingulate cortex (Cg)	0.063	0.416	0.176	0.273	–0.116	0.347
Cg (%)	–0.088	0.382	–0.154	0.300	0.044	0.441

Data shown are correlation coefficients (Pearson's r) and p-values (two-tailed t-test) for both absolute and relative volumes (mm^3). Values in bold indicate a trend-level statistical significance ($p<0.05$ uncorrected for multiple comparisons).

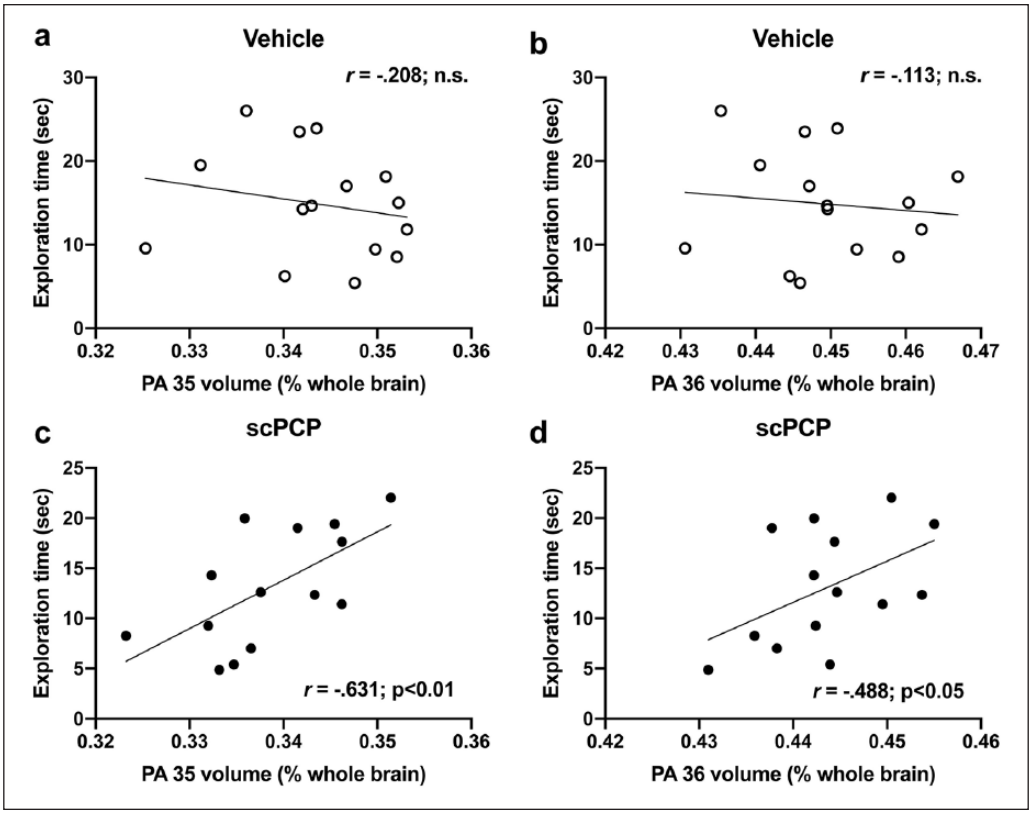

Figure 5. No relationship between the relative volumes of the perirhinal cortex areas 35 and 36 and time spent exploring the novel object in vehicle controls (Figure 5a and 5b). In contrast, a positive correlation is observed in sub-chronic phencyclidine (scPCP) rats (Figure 5c and 5d). Data shown are exploration time for the novel object (seconds) and relative volume (as percetnage of total brain) for each animal in each group. The *r* and *p*-values indicated reflect both the data from a Pearson's correlation. PA: perirhinal cortex area.

Discussion

The main findings of the current study are that in female Lister Hooded rats, scPCP exposure induced the expected deficit in object exploration time at one week after drug exposure, which was sustained out to six weeks. Although DI was clearly reduced in the scPCP rats this, however, failed to reach statistical significance. Exposure to scPCP also resulted in an elevated LMA response to an acute PCP challenge. At six weeks after cessation of treatment, scPCP rats had significantly reduced global brain volume, which lacked any apparent regional specificity, since all significant differences in volume were lost after a correction for global brain volumes, strongly suggesting an allometric effect (smaller brain, smaller regional volumes). At six weeks post-treatment, there were no significant correlations between the volumes of *a priori* selected brain ROIs and behavioural measures recorded in the NOR task in vehicle-controls. In contrast, the relative volumes of the perirhinal cortex areas 35 and 36 were positively correlated with time spent exploring the novel object in the scPCP group, such that scPCP rats with smaller relative volumes of these structures spent less time exploring the novel object.

These data replicate previous reports of sustained impairment in a simple cognitive task based on NOR using this scPCP-dosing regimen (Leger et al., 2015, McLean et al., 2011). It is important to note that scPCP rats failed to discriminate the novel from familiar object in retention at both time-points, shown as no significant difference between novel and familiar object exploration times, unlike the vehicle group. The DI which represents a ratio of this discrimination, however, failed to achieve statistical significance, when comparing scPCP to vehicle controls. This most likely reflects a relatively low value seen in the vehicle animals, rather than the absence of reduced DI in the scPCP rats (for reference please refer to values for vehicle-treated animals in (McLean et al., 2011)). Although the validity of this task for assessing cognitive deficits in the context of schizophrenia has been challenged (Pratt et al., 2012), we suggest it still represents a useful, non-food rewarded task to assess recognition memory deficits that are broadly applicable to a range of central nervous system (CNS) disorders (Grayson et al., 2015). Importantly, we and others have previously shown that this scPCP dosing regimen also induces long-lasting impairments in cognitive domains with greater relevance for schizophrenia, including executive function, problem solving and reasoning, attention, vigilance and aspects of negative symptoms including social behaviour and affect (Cadinu et al., 2018; Neill et al., 2010; Neill et al., 2014).

In contrast to this extensive behavioural validation, only a single published study to date has examined the impact of scPCP on brain volumes (Barnes et al., 2014). Furthermore, this was not done in the same animals that also underwent behavioural testing, and thus any functional relevance of the structural MRI changes may only be inferred and was not directly tested. Nonetheless, Barnes and colleagues (Barnes et al., 2014) reported

significant bilateral reductions in grey matter density in the anterior cingulate cortex (ACC), ventral striatum (VS), amygdaloid nucleus and hippocampal formation accompanied by lateralised reductions in the thickness of the somatosensory and insula cortices. These findings have clear face validity for structural brain alterations commonly reported in patients with schizophrenia (Barnes et al., 2014). These data are also consistent with MRI findings in mice exposed sub-chronically to other NMDAR antagonists such as MK-801, in which grey matter volume reductions and microstructural alterations of cerebral white matter measured using diffusion tensor imaging (DTI) have also been previously reported (Wu et al., 2016; Xiu et al., 2014; Xiu et al., 2015). Our data extend these findings to suggest that after a six-week washout period the female LH rat brain volume is globally reduced in the scPCP group compared to saline controls. The combined ABS and TBM analysis approach revealed that this reflects widespread significant regional differences in the apparent absolute volume of several cortical and sub-cortical brain regions in scPCP-exposed rats. Notably, these include the same regions that are affected at seven days post-scPCP in males (Barnes et al., 2014). However, our analysis reveals that when relative volumes (corrected for global brain volume changes) are compared, there were no longer any statistically significant differences in either cortical or sub-cortical regional brain volumes between scPCP and saline-exposed rats, after correcting for multiple comparisons. These observations suggest a lack of regional specificity in brain-volume changes and that the widespread absolute volume changes most likely reflect an allometric effect due to the overall global brain-volume reduction following scPCP exposure. These data would however be consistent with a recent report suggesting that brain-volume changes in a large clinical MRI data set (n=2668 individuals with a diagnosis of schizophrenia, bipolar disorder or attention-deficit/hyperactivity disorder as compared to healthy controls) are strongly associated with global brain and intracranial volumes (Schwarz et al., 2019). Nonetheless, our data also show that the relative volumes of a small number of brain ROIs remained differentially affected by scPCP-exposure, albeit only at trend-level significance ($p<0.05$ uncorrected for multiple comparisons). These included decreases in the apparent relative volumes of the lateral somatosensory and posterior parietal cortex. Whilst we cannot exclude the possibility that these results are Type-I errors, these ROIs are consistent with the anatomical location of cortical thickness deficits reported in the previous structural MRI analysis of male scPCP-exposed rats (Barnes et al., 2014). The magnitude of these relative volume reductions is also small, (range: 2–3%), which *in silico* experiments on MR image registration sensitivity suggest would be unlikely to survive a conservative multiple comparisons correction, as is the case here (van Eede et al., 2013). Measures of cortical thickness may also reflect a more sensitive and topographically relevant index of subtle anatomical brain remodelling in both humans and preclinical models, respectively (Lerch et al., 2008a; van Erp et al., 2018; Vernon et al., 2014).

Taken together, whilst there are commonalities in the two MRI data sets, there are also clear differences. In this respect, key methodological differences between the two studies should be noted. First, Barnes and colleagues (2014) used male Lister Hooded rats, whereas we have used females. The female rat brain may be more sensitive to PCP; hence we observe proportionally greater neuroanatomical effects. Supporting this hypothesis, female rats are more sensitive to scPCP, with differential pharmacokinetic effects (Shelnutt et al., 1999), greater impairments in performance in an attention-set-shifting task and increased PCP-associated neurotoxicity, including widespread reductions in brain-derived neurotrophic factor (BDNF) in several brain regions post-scPCP (Fix et al., 1995; Snigdha et al., 2011). Second, a higher dose of 5 mg/kg was used, as compared to the 2 mg/kg dose in our study due to pharmacokinetic differences between male and female rats (Shelnutt et al., 1999). Third, MR images were acquired after only one week of drug washout (Barnes et al., 2014) as compared to six weeks in the current study. It may be hypothesised that scPCP exposure initially leads to a region-specific anatomical remodelling of the rat brain, which may proceed to a more progressive course, resulting in global deficits with increasing time post-scPCP treatment. In support of this, we observe robust reductions in parvalbumin (PV) expression at six weeks post-scPCP treatment, but not earlier (Leger et al., 2015). Fourth, the MR images were analysed differently. Barnes and colleagues used voxel-based morphometry (VBM) (Barnes et al., 2014; Sawiak et al., 2009b), whilst we used TBM (Lau et al., 2008; Vernon et al., 2014). A key difference in these two methods is that VBM contains an additional series of steps to segment MR images into tissue classes (grey, white matter and CSF), whereas TBM does not (Sawiak et al., 2009b). It may be argued then, that the use of two different analysis methods could lead to differential results between our study and that of Barnes and colleagues (Barnes et al., 2014). To address this question, we refer to a direct comparison of these methods performed using high resolution *ex vivo* MR images acquired from a murine model of Huntington's disease (HD; R6/2 mutant) and their wild-type (WT) littermates (Sawiak et al., 2009a). This study demonstrates first, that a TBM analysis finds all of the results that a VBM analysis would. Second, TBM analysis identifies many additional regions that are significantly affected in terms of their volume, when comparing R6/2 to WT mice as compared to VBM (Sawiak et al., 2009a). This is not surprising since VBM uses the probability of grey matter as its statistical measure, whereas TBM uses the local volume change independent of tissue type (Sawiak et al., 2009a). Therefore using TBM and avoiding assumptions about tissue classes that can be challenging to separate in the rodent brain due to the relative paucity of white matter (Lau et al., 2008) may reveal more information. Put simply, whilst VBM and TBM find common changes, it may be argued that TBM is more sensitive, hence the greater number of significant voxels found in our study, at least using absolute volumes. Future longitudinal MRI studies in scPCP and saline-exposed rats of both sexes are now required to establish the sex-dependence, timing, nature (progressive or static) and any regional specificity of brain volume changes following scPCP exposure. A direct head-to-head comparison of VBM and TBM methodology in this study may also prove useful for the field.

A goal of this study was to explore whether there is any potential functional relevance of the observed brain volume reductions in scPCP rats. Hence, we tested for associations between MRI-derived brain volumes and behavioural measures extracted from the NOR task six weeks post-treatment. We focussed this analysis on nine *a priori*-selected brain ROIs from our MRI atlas, based on literature confirming a key role for these structures in object recognition memory (see Materials and methods section). We also included whole brain volume since this was globally reduced in the scPCP rats. This analysis revealed a trend-level correlation ($p<0.05$ uncorrected for multiple comparisons) between the relative volumes of the perirhinal cortex areas 35 and 36 and the time spent exploring the novel

object in scPCP, but not vehicle-treated, rats. These data are consistent with the established role of the perirhinal cortex in object recognition memory and novelty detection, based on lesioning and chemogenetic studies (Brown and Aggleton, 2001; Kinnavane et al., 2016; Morillas et al., 2017; Peters et al., 2018; Winters et al., 2008). Taken together, these data suggest there may well be functionally relevant links between the volumes of individual brain regions and behavioural performance in this scPCP model. Changes in connectivity between brain regions are also clearly important in this context. Indeed, brain network changes beyond the perirhinal cortex are clearly implicated in object recognition memory formation (Tanimizu et al., 2018). Furthermore, the importance of looking at networks is evidenced by elegant studies combining LCGU and functional connectivity analysis, which have linked abnormalities in functional brain networks post-scPCP to impaired cognitive performance (Dawson et al., 2010; Dawson et al., 2014; Dawson et al., 2015). To the best of our knowledge however, the perirhinal area was not included in these studies. Future studies are now needed to replicate and extended these findings including more relevant behavioural tests, such as those of passive and active attention, previously reported to be deficient in male rats exposed to scPCP (Barnes et al., 2014). We did not assess any correlation to LMA as this was temporally separated from the MR image acquisition. In the context of NOR, both male and female rats show robust deficits in this cognitive task, provided the dosing schedule is adjusted to account for these sex-specific pharmacokinetic effects of PCP (see Janhunen et al., 2015 for an extensive review).

Mechanistic studies are also required to understand the cellular basis of brain volume changes in this scPCP model and how this might influence the relationship to behavioural data. Cognitive performance and memory processes have been suggested to be associated with remodelling of dendritic spine density on pyramidal neurons, including in the prefrontal cortex (PFC). Specifically, a reduction in dendritic spine density on these primary neurons may contribute to cognitive dysfunction (Kasai et al., 2010). In support of this, there are correlations between the loss of asymmetric spine synapses in the primate PFC and the emergence of cognitive dysfunction during ageing (Dumitriu et al., 2010; Peters et al., 2008). Decreased density of PFC pyramidal neuron dendritic spines, suggestive of spine loss, is also reported from *post-mortem* studies of PFC brain tissue from schizophrenia patients (Glantz and Lewis, 2001). Furthermore, two prior studies have found evidence for decreased dendritic spine density in the PFC following scPCP treatment in rats, which persists for at least four weeks (Elsworth et al., 2011; Hajszan et al., 2006). No such data are however available in the perirhinal cortex following scPCP administration. At least in the rodent brain, changes in neuronal dendritic spine density are suggested to correlate with apparent brain volume changes detected using voxel-wise morphometry analysis of MR images (Keifer et al., 2015). Whilst a change in spine density would be predicted to contribute, at least in part, to the apparent volume changes detectable by MRI, it should be remembered that the latter could also simply be an epiphenomena of this spine loss and thus not related to the behavioural changes. Moreover, apparent changes in brain volume as measured using MRI (which, it should be remembered does not measure brain structure directly) may also reflect changes in several other cellular compartments, including glia, blood vessels and myelin content (Stolp et al., 2018; Zatorre et al., 2012), which have yet to be investigated in this scPCP model. Longitudinal MRI and behavioural studies in larger sample sizes, of both sexes, with detailed *post-mortem* follow-up including assessments of spine density are therefore required to map the cellular correlates of brain volume changes and identify which of these mediates the link to behavioural deficits in specific brain regions such as the perirhinal cortex. In this context, the work of Wu and colleagues (2016) may suggest some important leads. Specifically, following chronic exposure of mice to the NMDA-receptor antagonist MK-801, they report findings of increased numbers of necrotic cells in brain regions with reduced grey matter volume detectable by MRI, at least at trend level ($p<0.01$ uncorrected) (Wu et al., 2016). Furthermore, in specific sub-fields of the hippocampus, which also demonstrated apparent reduced grey matter volume (as detected by MRI), there was evidence for a reduction in the number of PV immunopositive interneurons and decreased dendritic spine complexity and density on pyramidal neurons (Wu et al., 2016). In the white matter tracts, of these animals, in which both reduced volume and microstructural changes (increased fractional anisotropy) are detectable by MRI, they provide evidence for decreased myelin basic protein immunoreactivity suggestive of demyelination (Wu et al., 2016), as reported previously in this model (Xiu et al., 2014; Xiu et al., 2015). As already indicated, such future studies should also include testing for relationships between not only brain structure, but also function, (Dawson et al., 2010) and other cognitive domains that are impaired in the scPCP model, particularly given that human studies suggest complex relationships between brain anatomy and cognitive performance across different tasks and domains, including studies in patients with schizophrenia (Brandt et al., 2015; Heinrichs et al., 2017; Jirsaraie et al., 2018; Karnik-Henry et al., 2012; Massey et al., 2017,).

Conclusion

In summary, our data confirm our previous work showing that scPCP exposure leads to long-lasting behavioural deficits in the NOR task when comparing object exploration time directly. We show for the first time that in the female Lister Hooded rat brain these are accompanied by global brain volume reductions that are without apparent regional specificity. The latter may reflect either enhanced sensitivity to scPCP in female rats compared to males, which show more regionally selective grey matter volume changes, or that progressive brain volume loss occurs at a later time-point following scPCP exposure. Our analyses also suggest that some of these phenomena are related, specifically, the relative volumes of the perirhinal cortex are positively correlated with novel object exploration time at six weeks only in scPCP rats. These data provide a clear rationale for future *in vivo* longitudinal, multi-modal MRI studies; incorporating cognitive testing and detailed *post-mortem* analysis following scPCP exposure. Such studies have the potential to establish a set of non-invasive, cross-species biomarkers to increase the predictive validity of testing novel therapeutics with pro-cognitive actions in the scPCP model for cognitive impairments in schizophrenia and other serious mental illnesses.

Acknowledgements

The authors acknowledge the expert help of the Biomarker Research and Imaging in Neuroscience (BRAIN) centre at King's College London and the UK Government Research Infrastructure Award for supporting the 9.4T preclinical MRI scanner at King's College London. MR images used in this study are freely available upon reasonable request to the corresponding author.

Declaration of conflicting interests

The author(s) declared the following potential conflicts of interest with respect to the research, authorship, and/or publication of this article: ACV declares previously receiving investigator-initiated research funding from F. Hoffman La Roche Ltd. The remaining authors declare no conflicts of interest.

Funding

The author(s) disclosed receipt of the following financial support for the research, authorship and/or publication of this article: ACV acknowledges financial support for this study from the Medical Research Council (New Investigator Research Grant (NIRG), MR/N025377/1). The work (at King's College, London) was also supported by the Medical Research Council (MRC) Centre grant (MR/N026063/1). The work (at the University of Manchester) was funded by b-neuro, and by a President's Doctoral Scholarship awarded to ND. The funders had no role in the decision to publish this study.

Supplemental material

Supplemental material for this article is available online.

ORCID iD

Anthony C Vernon https://orcid.org/0000-0001-7305-1069

References

Abdul-Monim Z, Neill JC and Reynolds GP (2007) Sub-chronic psychotomimetic phencyclidine induces deficits in reversal learning and alterations in parvalbumin-immunoreactive expression in the rat. *J Psychopharmacol* 21: 198–205.

Barnes SA, Sawiak SJ, Caprioli D, et al. (2014) Impaired limbic corticostriatal structure and sustained visual attention in a rodent model of schizophrenia. *Int J Neuropsychopharmacol* 18: pii: pyu010. doi: 10.1093/ijnp/pyu010.

Bora E and Pantelis C (2015) Meta-analysis of cognitive impairment in first-episode bipolar disorder: Comparison with first-episode schizophrenia and healthy controls. *Schizophr Bull* 41: 1095–1104.

Bortolato B, Miskowiak KW, Kohler CA, et al. (2015) Cognitive dysfunction in bipolar disorder and schizophrenia: A systematic review of meta-analyses. *Neuropsychiatr Dis Treat* 11: 3111–3125.

Brandt CL, Doan NT, Tonnesen S, et al. (2015) Assessing brain structural associations with working-memory related brain patterns in schizophrenia and healthy controls using linked independent component analysis. *Neuroimage Clin* 9: 253–263.

Brown MW and Aggleton JP (2001) Recognition memory: What are the roles of the perirhinal cortex and hippocampus? *Nat Rev Neurosci* 2: 51–61.

Brugger SP and Howes OD (2017) Heterogeneity and homogeneity of regional brain structure in schizophrenia a meta-analysis. *JAMA Psychiatry* 74: 1104–1111.

Cadinu D, Grayson B, Podda G, et al. (2018) NMDA receptor antagonist rodent models for cognition in schizophrenia and identification of novel drug treatments, an update. *Neuropharmacology* 142: 41–62.

Chang EH and Huerta PT (2012) Neurophysiological correlates of object recognition in the dorsal subiculum. *Front Behav Neurosci* 6: 46.

Chesters R, Stone JM, Wood TC, et al. (2017) Neuroadaptations to chronic ketamine exposure: A parallel human and mouse MRI imaging study. *Biol Psychiatry* 81: S118.

Crum WR, Sawiak SJ, Chege W, et al. (2017) Evolution of structural abnormalities in the rat brain following in utero exposure to maternal immune activation: A longitudinal in vivo MRI study. *Brain Behav Immun* 63: 50–59.

Dawson N, Higham DJ, Morris BJ, et al. (2010) Alterations in functional brain network structure induced by subchronic phencyclidine (PCP) treatment parallel those seen in schizophrenia. *J Psychopharmacol* 24: a18.

Dawson N, Morris BJ and Pratt JA (2015) Functional brain connectivity phenotypes for schizophrenia drug discovery. *J Psychopharmacol* 29: 169–177.

Dawson N, Xiao XL, Mcdonald M, et al. (2014) Sustained NMDA receptor hypofunction induces compromised neural systems integration and schizophrenia-like alterations in functional brain networks. *Cereb Cortex* 24: 452–464.

Dempster K, Norman R, Theberge J, et al. (2017) Cognitive performance is associated with gray matter decline in first-episode psychosis. *Psychiatry Res Neuroimaging* 264: 46–51.

Dumitriu D, Hao J, Hara Y, et al. (2010) Selective changes in thin spine density and morphology in monkey prefrontal cortex correlate with aging-related cognitive impairment. *J Neurosci* 30: 7507–7515.

Edward Roberts R, Curran HV, Friston KJ, et al. (2014) Abnormalities in white matter microstructure associated with chronic ketamine use. *Neuropsychopharmacology* 39: 329–38.

Elsworth JD, Morrow BA, Hajszan T, et al. (2011) Phencyclidine-induced loss of asymmetric spine synapses in rodent prefrontal cortex is reversed by acute and chronic treatment with olanzapine. *Neuropsychopharmacology* 36: 2054–2061.

Fix AS, Wozniak DF, Truex LL, et al. (1995) Quantitative analysis of factors influencing neuronal necrosis induced by MK-801 in the rat posterior cingulate/retrosplenial cortex. *Brain Res* 696: 194–204.

Genovese CR, Lazar NA and Nichols T (2002) Thresholding of statistical maps in functional neuroimaging using the false discovery rate. *Neuroimage* 15: 870–878.

Gilbert PE and Kesner RP (2003) Recognition memory for complex visual discriminations is influenced by stimulus interference in rodents with perirhinal cortex damage. *Learn Mem* 10: 525–530.

Glantz LA and Lewis DA (2001) Dendritic spine density in schizophrenia and depression. *Arch Gen Psychiatry* 58: 203–203.

Gozzi A, Large CH, Schwarz A, et al. (2008) Differential effects of antipsychotic and glutamatergic agents on the phMRI response to phencyclidine. *Neuropsychopharmacology* 33: 1690–1703.

Grayson B, Idris NF and Neill JC (2007) Atypical antipsychotics attenuate a sub-chronic PCP-induced cognitive deficit in the novel object recognition task in the rat. *Behav Brain Res* 184: 31–38.

Grayson B, Leger M, Piercy C, et al. (2015) Assessment of disease-related cognitive impairments using the novel object recognition (NOR) task in rodents. *Behav Brain Res* 285: 176–193.

Green MF (2006) Cognitive impairment and functional outcome in schizophrenia and bipolar disorder. *J Clin Psychiatry* 67(Suppl 9): 3–8; discussion 36–42.

Haijma SV, Van Haren N, Cahn W, et al. (2013) Brain volumes in schizophrenia: A meta-analysis in over 18 000 subjects. *Schizophr Bull* 39: 1129–1138.

Hajszan T, Leranth C and Roth RH (2006) Subchronic phencyclidine treatment decreases the number of dendritic spine synapses in the rat prefrontal cortex. *Biol Psychiatry* 60: 639–644.

Hamburg H, Trossbach SV, Bader V, et al. (2016) Simultaneous effects on parvalbumin-positive interneuron and dopaminergic system development in a transgenic rat model for sporadic schizophrenia. *Sci Rep* 6: 34946.

Heinrichs RW, Pinnock F, Parlar M, et al. (2017) Cortical thinning in network-associated regions in cognitively normal and below-normal range schizophrenia. *Schizophr Res Treatment* 2017: 1–7.

Janhunen SK, Svärd H, Talpos J, et al. (2015) The subchronic phencyclidine rat model: Relevance for the assessment of novel therapeutics for cognitive impairment associated with schizophrenia. *Psychopharmacology (Berl)* 232: 4059–4083.

Jirsaraie RJ, Sheffield JM and Barch DM (2018) Neural correlates of global and specific cognitive deficits in schizophrenia. *Schizophr Res* 201: 237–242.

Karnik-Henry MS, Wang L, Barch DM, et al. (2012) Medial temporal lobe structure and cognition in individuals with schizophrenia and in their non-psychotic siblings. *Schizophr Res* 138: 128–135.

Kasai H, Fukuda M, Watanabe S, et al. (2010) Structural dynamics of dendritic spines in memory and cognition. *Trends Neurosci* 33: 121–129.

Keifer OP, Hurt RC, Gutman DA, et al. (2015) Voxel-based morphometry predicts shifts in dendritic spine density and morphology with auditory fear conditioning. *Nat Commun* 6: 7582.

Kim JS, Kornhuber HH, Schmid-Burgk W, et al. (1980) Low cerebrospinal fluid glutamate in schizophrenic patients and a new hypothesis on schizophrenia. *Neurosci Lett* 20: 379–382.

Kinnavane L, Amin E, Olarte-Sanchez CM, et al. (2016) Detecting and discriminating novel objects: The impact of perirhinal cortex disconnection on hippocampal activity patterns. *Hippocampus* 26: 1393–1413.

Krystal JH, Karper LP, Seibyl JP, et al. (1994) Subanesthetic effects of the noncompetitive nmda antagonist, ketamine, in humans. Psychotomimetic, perceptual, cognitive, and neuroendocrine responses. *Arch Gen Psychiatry* 51: 199–214.

Lahti AC, Holcomb HH, Medoff DR, et al. (1995a) Ketamine activates psychosis and alters limbic blood flow in schizophrenia. *Neuroreport* 6: 869–872.

Lahti AC, Koffel B, Laporte D, et al. (1995b) Subanesthetic doses of ketamine stimulate psychosis in schizophrenia. *Neuropsychopharmacology* 13: 9–19.

Lau JC, Lerch JP, Sled JG, et al. (2008) Longitudinal neuroanatomical changes determined by deformation-based morphometry in a mouse model of Alzheimer's disease. *Neuroimage* 42: 19–27.

Leger M, Alvaro G, Large C, et al. (2015) AUT6, a novel Kv3 channel modulator, reverses cognitive and neurobiological dysfunction in a rat model of relevance to schizophrenia symptomatology. *Eur Neuropsychopharmacol* 25: S480.

Lerch JP, Carroll JB, Dorr A, et al. (2008a) Cortical thickness measured from MRI in the YAC128 mouse model of Huntington's disease. *Neuroimage* 41: 243–251.

Lerch JP, Carroll JB, Spring S, et al. (2008b) Automated deformation analysis in the YAC128 Huntington disease mouse model. *Neuroimage* 39: 32–39.

Lerch JP, Gazdzinski L, Germann J, et al. (2012) Wanted dead or alive? The tradeoff between in-vivo versus ex-vivo MR brain imaging in the mouse. *Front Neuroinform* 6: 6.

Liao Y, Tang J, Corlett PR, et al. (2011) Reduced dorsal prefrontal gray matter after chronic ketamine use. *Biol Psychiatry* 69: 42–48.

Liao Y, Tang J, Ma M, et al. (2010) Frontal white matter abnormalities following chronic ketamine use: A diffusion tensor imaging study. *Brain* 133: 2115–2122.

Massey SH, Stern D, Alden EC, et al. (2017) Cortical thickness of neural substrates supporting cognitive empathy in individuals with schizophrenia. *Schizophr Res* 179: 119–124.

McLean SL, Grayson B, Idris NF, et al. (2011) Activation of alpha7 nicotinic receptors improves phencyclidine-induced deficits in cognitive tasks in rats: Implications for therapy of cognitive dysfunction in schizophrenia. *Eur Neuropsychopharmacol* 21: 333–343.

McLean SL, Harte MK, Neill JC, et al. (2017) Dopamine dysregulation in the prefrontal cortex relates to cognitive deficits in the sub-chronic PCP-model for schizophrenia: A preliminary investigation. *J Psychopharmacol* 31: 660–666.

Moghaddam B and Javitt D (2012) From revolution to evolution: The glutamate hypothesis of schizophrenia and its implication for treatment. *Neuropsychopharmacology* 37: 4–15.

Morillas E, Gomez-Chacon B and Gallo M (2017) Flavor and object recognition memory impairment induced by excitotoxic lesions of the perirhinal cortex. *Neurobiol Learn Mem* 144: 230–234.

Neill JC, Barnes S, Cook S, et al. (2010) Animal models of cognitive dysfunction and negative symptoms of schizophrenia: Focus on nmda receptor antagonism. *Pharmacol Ther* 128: 419–432.

Neill JC, Harte MK, Haddad PM, et al. (2014) Acute and chronic effects of NMDA receptor antagonists in rodents, relevance to negative symptoms of schizophrenia: A translational link to humans. *Eur Neuropsychopharmacol* 24: 822–835.

Papp EA, Leergaard TB, Calabrese E, et al. (2014) Waxholm Space atlas of the Sprague Dawley rat brain. *Neuroimage* 97: 374–386.

Peters A, Sethares C and Luebke JI (2008) Synapses are lost during aging in the primate prefrontal cortex. *Neuroscience* 152: 970–981.

Peters J, Scofield MD and Reichel CM (2018) Chemogenetic activation of the perirhinal cortex reverses methamphetamine-induced memory deficits and reduces relapse. *Learn Mem* 25: 410–415.

Pratt J, Winchester C, Dawson N, et al. (2012) Advancing schizophrenia drug discovery: Optimizing rodent models to bridge the translational gap. *Nat Rev Drug Discov* 11: 560–579.

Reynolds GP and Neill JC (2016) Modelling the cognitive and neuropathological features of schizophrenia with phencyclidine. *J Psychopharmacol* 30: 1141–1144.

Richetto J, Chesters R, Cattaneo A, et al. (2017) Genome-wide transcriptional profiling and structural magnetic resonance imaging in the maternal immune activation model of neurodevelopmental disorders. *Cereb Cortex* 27: 3397–3413.

Sawiak SJ, Wood NI, Williams GB, et al. (2009a) Deformation-based morphometry in the R6/2 Huntington's disease mouse brain. *Proc Int Soc Magn Reson Imaging* 17: 545.

Sawiak SJ, Wood NI, Williams GB, et al. (2009b) Voxel-based morphometry in the R6/2 transgenic mouse reveals differences between genotypes not seen with manual 2D morphometry. *Neurobiol Dis* 33: 20–27.

Schwarz E, Doan NT, Pergola G, et al. (2019) Reproducible grey matter patterns index a multivariate, global alteration of brain structure in schizophrenia and bipolar disorder. *Transl Psychiatry* 9: 12.

Shelnutt SR, Gunnell M and Owens SM (1999) Sexual dimorphism in phencyclidine in vitro metabolism and pharmacokinetics in rats. *J Pharmacol Exp Ther* 290: 1292–1298.

Snigdha S, Neill JC, McLean SL, et al. (2011) Phencyclidine (PCP)-induced disruption in cognitive performance is gender-specific and associated with a reduction in brain-derived neurotrophic factor (BDNF) in specific regions of the female rat brain. *J Mol Neurosci* 43: 337–345.

Stolp HB, Ball G, So PW, et al. (2018) Voxel-wise comparisons of cellular microstructure and diffusion-MRI in mouse hippocampus using 3D bridging of optically-clear histology with neuroimaging data (3D-BOND). *Sci Rep* 8: 4011.

Tanimizu T, Kono K and Kida S (2018) Brain networks activated to form object recognition memory. *Brain Res Bull* 141: 27–34.

Valdes-Hernandez PA, Sumiyoshi A, Nonaka H, et al. (2011) An in vivo MRI template set for morphometry, tissue segmentation, and fMRI localization in rats. *Front Neuroinform* 5: 26.

van Eede MC, Scholz J, Chakravarty MM, et al. (2013) Mapping registration sensitivity in MR mouse brain images. *Neuroimage* 82: 226–236.

van Erp TG, Hibar DP, Rasmussen JM, et al. (2016) Subcortical brain volume abnormalities in 2028 individuals with schizophrenia and 2540 healthy controls via the enigma consortium. *Mol Psychiatry* 21: 547–553.

van Erp TGM, Walton E, Hibar DP, et al. (2018) Cortical brain abnormalities in 4474 individuals with schizophrenia and 5098 control subjects via the enhancing neuro imaging genetics through meta analysis (ENIGMA) consortium. *Biol Psychiatry* 84: 644–654.

Vernon AC, Crum WR, Lerch JP, et al. (2014) Reduced cortical volume and elevated astrocyte density in rats chronically treated with antipsychotic drugs-linking magnetic resonance imaging findings to cellular pathology. *Biol Psychiatry* 75: 982–990.

Vernon AC, Natesan S, Modo M, et al. (2011) Effect of chronic antipsychotic treatment on brain structure: A serial magnetic resonance

imaging study with ex vivo and postmortem confirmation. *Biol Psychiatry* 69: 936–944.

Walton E, Hibar DP, Van Erp TGM, et al. (2018) Prefrontal cortical thinning links to negative symptoms in schizophrenia via the ENIGMA consortium. *Psychol Med* 48: 82–94.

Walton E, Hibar DP, Van Erp TGM, et al. (2017) Positive symptoms associate with cortical thinning in the superior temporal gyrus via the ENIGMA schizophrenia consortium. *Acta Psychiatrica Scandinavica* 135: 439–447.

Weible AP, Rowland DC, Pang R, et al. (2009) Neural correlates of novel object and novel location recognition behavior in the mouse anterior cingulate cortex. *J Neurophysiol* 102: 2055–2068.

Winters BD, Saksida LM and Bussey TJ (2008) Object recognition memory: Neurobiological mechanisms of encoding, consolidation and retrieval. *Neurosci Biobehav Rev* 32: 1055–1070.

Wood TC, Simmons C, Hurley SA, et al. (2016) Whole-brain ex-vivo quantitative MRI of the cuprizone mouse model. *PeerJ* 4: e2632.

Wu H, Wang X, Gao Y, et al. (2016) NMDA receptor antagonism by repetitive MK801 administration induces schizophrenia-like structural changes in the rat brain as revealed by voxel-based morphometry and diffusion tensor imaging. *Neuroscience* 322: 221–233.

Xiu Y, Kong XR, Zhang L, et al. (2014) White matter injuries induced by MK-801 in a mouse model of schizophrenia based on NMDA antagonism. *Anat Rec (Hoboken)* 297: 1498–1507.

Xiu Y, Kong XR, Zhang L, et al. (2015) The myelinated fiber loss in the corpus callosum of mouse model of schizophrenia induced by MK-801. *J Psychiatr Res* 63: 132–140.

Zatorre RJ, Fields RD and Johansen-Berg H (2012) Plasticity in gray and white: Neuroimaging changes in brain structure during learning. *Nat Neurosci* 15: 528–536.